Effects of the Pivot Position and Lubricant Flow Rate on the Behavior of Sector Shaped Tilting Pads Hydrodynamic Thrust Bearings

Vilmar Arthur Schwarz
Universidade Federal de Itajubá
vilmar@iem.efei.br

Paulo Fernandes Silva
MCT -Laboratório Nacional de Astrofísica
psilva@lna.br

William Martins Vicente
Universidade Federal de Itajubá
williampa@bol.com.br

José Célio Dias
Universidade Federal de Itajubá
jcelio@iem.efei.br

Mark J. Kuhn
Kingsbury Inc.
mjk@kingsbury.com

Abstract. *A six pads hydrodynamic thrust bearing consisted by pads with different pivot positions is experimentally and teoretically analysed. An ISO 32 viscosity grade lubricating oil is used with a wide range of flow rate, in order to obtain the minimum bearing operating temperatures for different conditions of applied loads, rotational speeds and oil cooling conditions. A brief description of the test rig is presented. Bearing friction torque and operating temperatures of the pads and the rotating collar are obtained. In the theoretical analysis the Reynolds equation is presented, giving the load capacity,oil flow rate and operating viscosity, friction torque and power losses within the bearing. Finally, a comparison between the experimental and theoretical results is presented.*

Keywords. *pivoted pads, temperature distribution, friction losses, oil flow rate, thrust bearing.*

1. Introduction

Extensive literature reviews on theoretical models and experimental works on the behavior of hydrodynamic thrust bearings are given by El-Saie & Fenner (1988) and Glavatskikh (2001). Comparison between theory and experiments is presented by Almqvist et all (2000), who also presents an interesting review on the literature.

Experimental data available in the literature have been usually taken from horizontal shaft thrust bearings with centrally pivoted or fixed pads. Friction power losses have been indirectly obtained from the so called “ hot oil carry over” which is a function of the difference between the temperatures of the lubricant at the inlet and the outlet positions in the bearing assembly, oil flow rate and specific heat (Gregory, 1974; Mikula, 1987).

Temperatures of the rotating collar have not been measured, exception made to Glavatskikh (2001), who measured temperatures of the rotating collar at two positions corresponding to 25% and 75% of the radial “contact” width and found insignificant difference between the two temperatures.

In the present work, friction torque is directly obtained by using a high precision torquemeter and the collar “surface” temperature is measured in the positions at 22%, 50% and 72% of the effective radial width. Axial temperatures of the collar are also measured and similarly, the pad temperature distribution is obtained, both in the undersurface “contact” area and in the axial direction along the pad thickness. Three pad pivot positions are investigated under various lubricant flow rate supplied to the bearing, in order to find out the operating conditions leading to minimum power losses or minimum operating temperatures.

2. Theoretical Analysis

2.1. Physical model

Figure 1 shows, schematically, a thrust bearing consisted by six sector pivoted pads with inner and outer radii R_i and R_o, respectively. The pivoting point of each pad is ahead of the center, such that the pads will operate with the ideal inclination. The pivot position is denoted by $?_p$ and R_p, while the sector angle is denoted by ?. The oil film thickness and the flow rate are denoted by h_{max} and Q_i at the leading edge of the pad, and by h_{min}= a and Q_o at the trailing edge. The circumferencial distance between the pad leading edge and the pivot position is denoted by L_p while L_s and L are the mean circumferential length and radial witdh of the pad, respectively. The pad taper is denoted by b= $h_{max} - h_{min}$ and the taper ratio is given by a/b. At the right side of Fig. (1), the pivot position is indicated both in cartesian and polar coordinates.

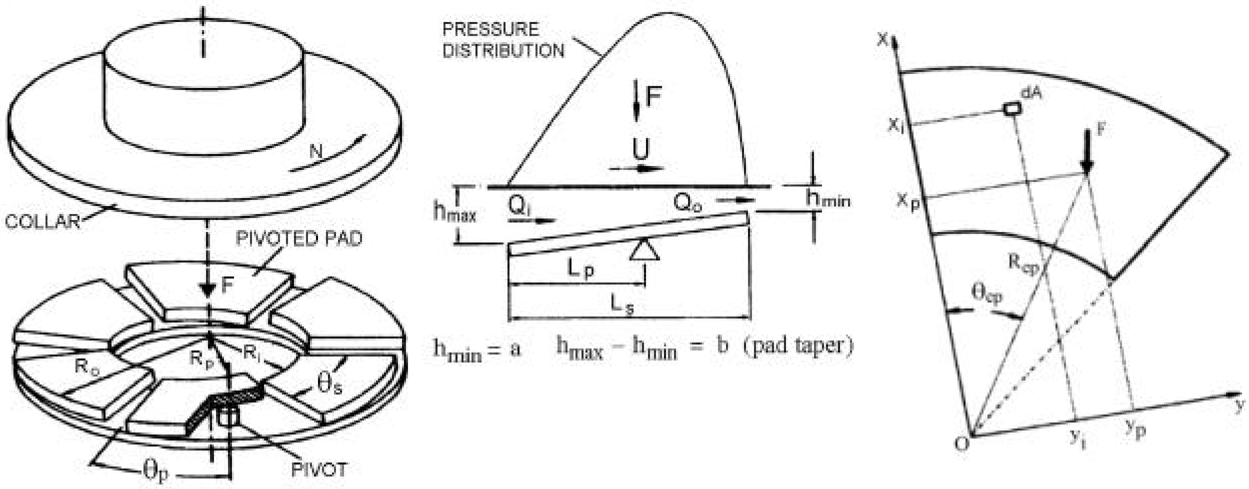

Figure 1. Scheme of a tilting pad hydrodynamic thrust bearing, pad pressure distribution and pad pressure center.

2.2. Reynolds Equation and Bearing Operating Parameters

The Reynolds equation and the most relevant bearing operating parameters, as adapted from Salles et al. (2001) may be written as follows:

Reynolds Equation. The non-dimensional Reynolds equation in polar coordinates is:

$$\frac{\partial}{\partial r}\left(r h^3 \frac{\partial p}{\partial r}\right)+\frac{1}{r}\frac{\partial}{\partial \theta}\left(h^3\frac{\partial p}{\partial \theta}\right)=12\pi r\left(\frac{R_o}{L}\right)^2\frac{\partial h}{\partial \theta} \tag{1}$$

where *r*,*h*, *p* and *?* are the dimensionless radius, oil film thickness, pressure and angular variable, while r_e,h_e , p_e and $?_e$ are the corresponding efective parameters, according to the following relationships:

$$r=\frac{r_e}{R_o}\,; \qquad h=\frac{h_e}{b}\,; \qquad p=\frac{p_e}{\eta N}\left(\frac{b}{L}\right)^2; \qquad \theta=\frac{\theta_e}{\theta_s} \tag{2}$$

In the above dimensionless parameters, the variables R_o, *?*, *N* and $?_s$ are the pad outer radius, lubricant viscosity within the oil film between the pad and the rotating collar, rotational speed and the pad angle, respectively.

Pressure distribution. By applying the finite difference method the pressure distribution on the pad is obtained from integration of the Reynolds equation, i. e.:

$$p_{i,j} = A1_{i,j}\,p_{i,j+1} + A2_{i,j}\,p_{i,j-1} + A3_{i,j}\,p_{i+1,j} + A4_{i,j}\,p_{i-1,j} + A5_{i,j} \tag{3}$$

Load carrying capacity. The hydrodynamic load carrying capacity *F* of a pad and its corresponding dimensionless parameter F_v are:

$$F=\int_{Ri}^{Ro}\int_0^{\theta_e} p_e r_e\, d\theta_e\, dr_e \quad ; \qquad F_v=\Delta r\,\Delta\theta\sum_{j=1}^{m}\sum_{i=1}^{n}P(i,j)\,r(j) \qquad \text{and} \qquad F=\eta N\frac{L^2}{b^2}R_o^2F_v \tag{4}$$

Pressure Center. Is the resultant load application point on the pad surface. Firstly, the point (x_p , y_p) shown in Fig. (1), at the right side, is determined by applying moments in relation to the x and y axis, as follows:

$$x_p=\frac{R_o}{F}\int_0^{\theta_s}\int_{\frac{R_i}{R_o}}^{1} p_{i,j}\,r_j^2\cos\theta_i\,dr\,d\theta \qquad \text{or} \qquad x_p=\frac{R_o}{F}\Delta r\Delta\theta\sum_{i=1}^{n}\sum_{j=1}^{m}p_{i,j}\,r_j^2\cos\theta_i \tag{5}$$

$$y_p=\frac{R_o}{F}\int_0^{\theta_s}\int_{\frac{R_i}{R_o}}^{1} p_{i,j}\,r_j^2\,\mathrm{sen}\,\theta_i\,dr\,d\theta \qquad \text{or} \qquad y_p=\frac{R_o}{F}\Delta r\Delta\theta\sum_{i=1}^{n}\sum_{j=1}^{m}p_{i,j}\,r_j^2\,\mathrm{sen}\,\theta_i \tag{6}$$

Therefore, from Fig. (1) the pressure center or pivot position, in polar coordinates, is given by:

$$R_{e_p} = \sqrt{x_p^2 + y_p^2} \quad ; \quad q_{e_p} = arctg \frac{y_p}{x_p} \quad \text{for} \quad q_p = \frac{q_{e_p}}{q_s} \quad ; \quad R_p = \frac{R_{e_p} - R_i}{R_o - R_i} \tag{7}$$

Friction power loss. Is the power loss due to the oil shear within the lubricant wedge between the pad and the rotating collar. Denoting by H_e and by H the effective and dimensionless power losses one may write:

$$H_e = H \frac{p P_e N R_o^4 a}{L^2} \quad ; \quad H = \left\{ p\, q_0 T \frac{b}{a} L_n\left(1 + \frac{b}{a}\right)\left[1 - \left(1 - \frac{L}{R_e}\right)^4\right] + s\, T \frac{b}{a}\left(\frac{L}{R_e}\right)^2 \right\} \tag{8}$$

where:

$$s = DrDq \sum_{j=1}^{m} \sum_{i=1}^{n} r_j h_i \frac{\P p}{\P q} \quad , \quad T = \frac{h N \left(L/b\right)^2}{P_e} \quad \text{and} \quad P_e = \frac{F}{A_p} \tag{9}$$

Note that in eq. (8) and (9) above, T is a dimensionless thrust factor and P_e is the pad specific pressure defined simply as the ratio between the thrust load F and the pad surface area A_p.

Lubricant flow rate. Four lubricant flow rates were taken into account, Q_i, Q_o, Q_{RI} and Q_{Ro} corresponding respectively to the oil flow rates at the leading edge, trailling edge, inner radius and outer radius of a pad, given as follows:

$$Q_i = p\, R_o N L b\left[\left(-1 + \frac{L}{2R_o}\right)\left(1 + \frac{a}{b}\right) + q_i\right] , \qquad q_i = \frac{L}{12pR_o} \int_{R_i/R_o}^{1} \frac{h^3}{r} \frac{\partial P}{\partial q}\bigg|_{q=0} dr \tag{10}$$

$$Q_o = p\, R_o N L b\left[\left(-1 + \frac{L}{2R_o}\right)\left(1 + \frac{a}{b}\right) + q_o\right] , \qquad q_o = \frac{L}{12pR_o} \int_{R_i/R_o}^{1} \frac{h^3}{r} \frac{\partial P}{\partial q}\bigg|_{q=q_s} dr \tag{11}$$

$$Q_{Ri} = p\, R_o N L b q_{Ri} \quad , \qquad q_{Ri} = \frac{1}{12p} \frac{L}{R_o} \int_0^{q_s} h^3 r \frac{\P p}{\P r}\bigg|_{r=R_i/R_o} dq \tag{12}$$

$$Q_{Ro} = p\, R_o N L b q_{Ro} \quad , \qquad q_{Ro} = \frac{-1}{12p} \frac{L}{R_o} \int_0^{q_s} h^3 r \frac{\P p}{\P r}\bigg|_{r=1} dq \tag{13}$$

3.Theoretical results

The computed data were obtained for the test bearing for a wide range of thrust load, rotational speed and pad taper ratio *a/b*. Table (1) shows some operating parameters of the thrust bearing, with the following input data to the computer program: R_i=57.15mm, R_o=114.3mm, *N= 33.33rps(2000rpm)*, *F=18kN* and three values of minimum oil film thickness, i.e., *a=20 µm, 26 µm and 32 µm* . The data given in Tab. (1) refer to a single pad, except by the values of power losses H and H_e and friction torque T_f , that correspond to the total bearing operating parameters. The friction torque, T_f, is simply calculated as the ratio between the power loss and the angular speed of the collar. The minimum value, *a=20 µm*, for the trailing edge oil film thickness in Tab. (1) was adopdet by assuming that the minimum oil film thickness in any hydrodynamic sliding bearing should be at least 10 times the combined surface roughness, which is usually less than *2 µm*. The experimental data given by Dadouche et al. (2000), for a rotational speed of 2000 rpm, show minimum film thickness values of 130 to 45 *µm* for thrust loads from 1 to 8 kN, respectively. However, this range of thrust load seems to be somewhat light, in respect to the *200 mm* outer diameter fixed pad bearing employed in Dadouche’s experimental work.

Table 1. Calculated thrust bearing operating parameters, for N=2000 rpm and F=18kN.

a/b	h_{min} (µm)	F_v	θ_p	Q_i (l/min)	Q_o (l/min)	? (mPa.s)	H	H_e (kW)	T_f (N.m)
0.2	20	3.518	0.714	2.788	0.884	5.995	2.623	1.209	5.771
	26	3.518	0.714	3.624	1.149	10.132	2.623	1.571	7.503
	32	3.518	0.714	4.461	1.414	15.348	2.623	1.934	9.234
0.3	20	1.949	0.681	2.089	0.833	4.809	2.429	1.119	5.345
	26	1.949	0.681	2.716	1.089	8.127	2.429	1.455	6.948
	32	1.949	0.681	3.342	1.333	12.310	2.429	1.791	8.552
0.4	20	1.221	0.669	1.735	0.799	4.317	2.397	1.104	5.273
	26	1.221	0.669	2.255	1.039	7.296	2.397	1.436	6.855
	32	1.221	0.669	2.776	1.279	11.051	2.397	1.767	8.437
0.5	20	0.826	0.639	1.520	0.775	4.087	2.430	1.120	5.346
	26	0.826	0.639	1.976	1.007	6.906	2.430	1.456	6.950
	32	0.826	0.639	2.432	1.239	10.462	2.430	1.792	8.554
0.6	20	0.588	0.625	1.375	0.757	3.982	2.497	1.150	5.492
	26	0.588	0.625	1.787	0.983	6.730	2.497	1.495	7.140
	32	0.588	0.625	2.200	1.210	10.195	2.497	1.841	8.788
0.7	20	0.436	0.614	1.271	0.742	3.948	2.582	1.190	5.681
	26	0.436	0.614	1.652	0.964	6.673	2.582	1.547	7.385
	32	0.436	0.614	2.033	1.186	10.108	2.582	1.904	9.089
0.8	20	0.333	0.605	1.192	0.730	3.958	2.680	1.235	5.896
	26	0.333	0.605	1.550	0.949	6.689	2.680	1.605	7.664
	32	0.333	0.605	1.907	1.168	10.132	2.680	1.976	9.433
0.9	20	0.261	0.597	1.130	0.720	3.996	2.785	1.284	6.128
	26	0.261	0.597	1.469	0.936	6.753	2.785	1.669	7.967
	32	0.261	0.597	1.808	1.152	10.229	2.785	2.054	9.805
1.0	20	0.208	0.590	1.081	0.712	4.053	2.897	1.335	6.374
	26	0.208	0.590	1.409	0.925	6.850	2.897	1.735	8.286
	32	0.208	0.590	1.729	1.139	10.376	2.897	2.136	10.198
1.1	20	0.169	0.584	1.040	0.705	4.125	3.012	1.388	6.628
	26	0.169	0.590	1.352	0.916	6.971	3.012	1.805	8.616
	32	0.169	0.590	1.664	1.128	10.560	3.012	2.221	10.605
1.2	20	0.139	0.579	1.006	0.699	4.208	3.131	1.443	6.889
	26	0.139	0.579	1.307	0.908	7.111	3.131	1.876	8.956
	32	0.139	0.579	1.609	1.118	10.772	3.131	2.309	11.022

As shown in Tab. (1) and in Fig. (2), friction power loss and friction torque show minimum values for pads with a taper ratio of about 0.4, which corresponds to a pad pivoted at an angle $?_p$ equal to about 66% of the pad sector angle, $?_s$, as can be seen from Tab. (1). From this theoretical conclusion, a set of six pads with such a pivot position was specially manufactured, for the experimental analysis described in Section 5.

Figure 2 shows the variation of computed friction torque against pad taper ratio, for four values of the minimum oil film thickness between each pad and the rotating collar. As expected, when the load and the speed are kept constant, the higher the oil film thickness, the higher the bearing operating torque. This aspect shall be further discussed in the paper, simultaneously with the experimentally measured friction torque and with the required operating viscosity of the lubricating oil, from Fig. (3).

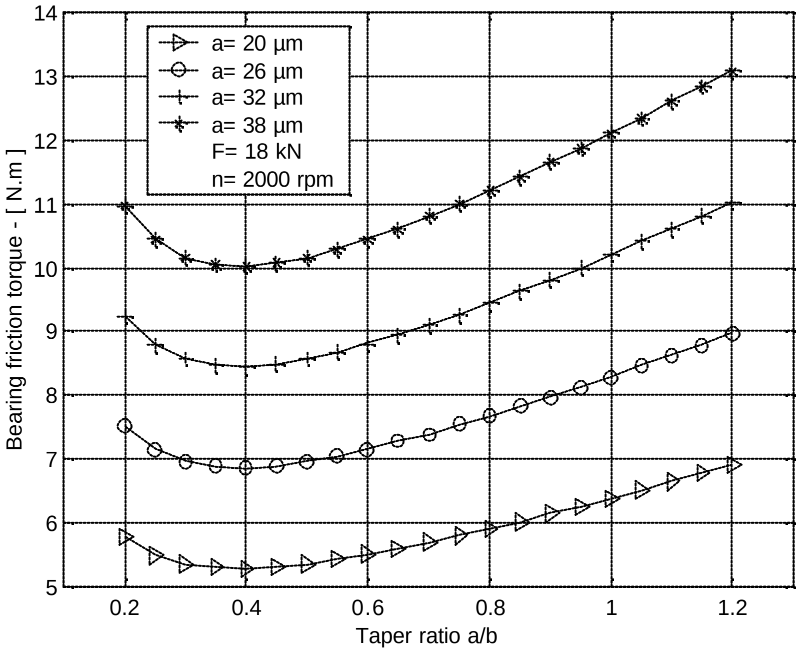

Figure 2. Computed bearing friction torque versus both the pad taper ratio and oil film thickness.

Figure 3 shows the mean viscosity of the lubricant oil within the oil film stablished between the bearing pads and the rotating collar. Four different values of the oil film thickness between the rotating collar and the trailing edge of the pads were taken into account, as shown in the legend of the figure. It can be seen that the thicker the oil film, the higher and more dependent on the taper ratio is the corresponding operational viscosity of the lubricant.

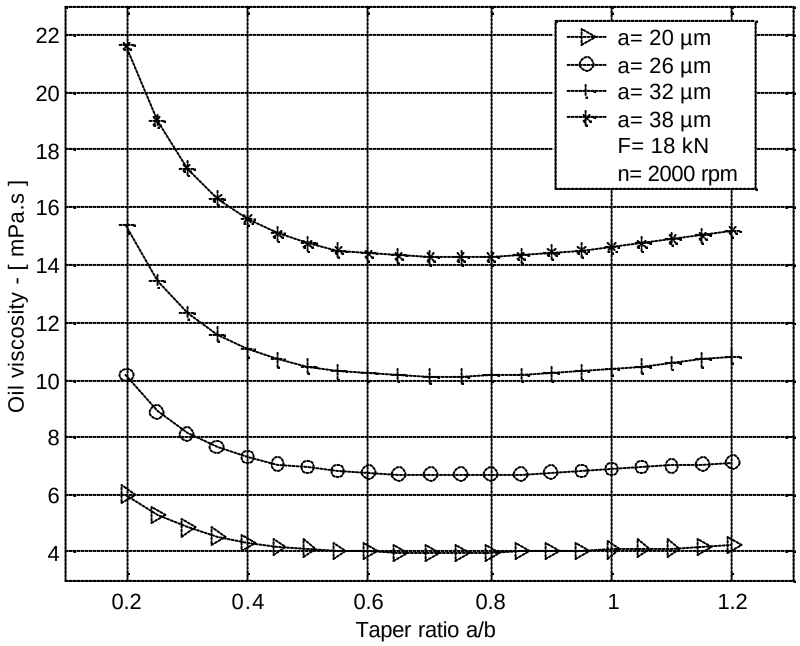

Figure 3. Mean operating viscosity of the lubricant oil at the average temperature of the oil film between each pad and the rotating collar.

Figure 4 shows the required operating viscosity of the oil in order to maintain a 20 µm film thickness at the trailing edge of each pad, for the thrust loads shown in the legend and rotational speed ranging from 1000 to 3000 rpm. It is evident that the required operating viscosity of the oil, at an average oil film temperature, is lower for higher rotational speeds and higher for heavier loads.

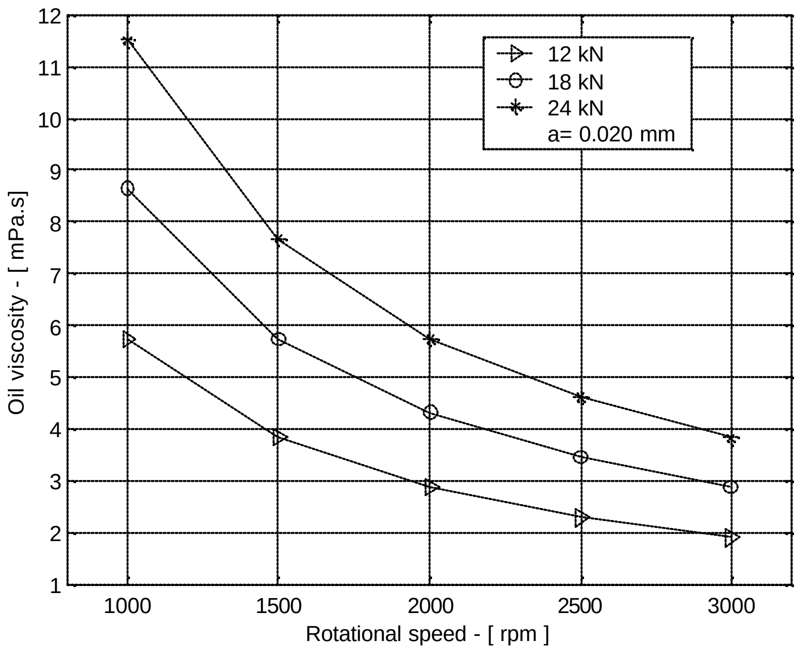

Figure 4. Operational viscosity of the lubricating oil versus rotational speed.

Figure 5 shows, for a 66% pivoted pad, that the computed oil flow rates at the leading and the trailing edge of the pad increase linearly with the rotational speed. Most of the available experimental data in literature, such as Glavatskikh (2001), are given for a constant oil flow rate to the bearing and various rotational speeds. However, as can be seen from Fig. (5), the higher the rotational speed, the higher the oil flow rate self pumped by the bearing.

It is important to have in mind that for a vertical shaft thrust bearing, similar to that of the present paper, some kind of "oil bath lubrication" pertains, and, roughly, one could assume that the oil leaving one pad is carried by the collar to the next pad. In this way, the required oil flow rate to the bearing could be considered as the difference between Q_i and Q_o, given in Tab. (1) and in Fig. (5), multipllied by the number of pads from which the bearing is composed of.

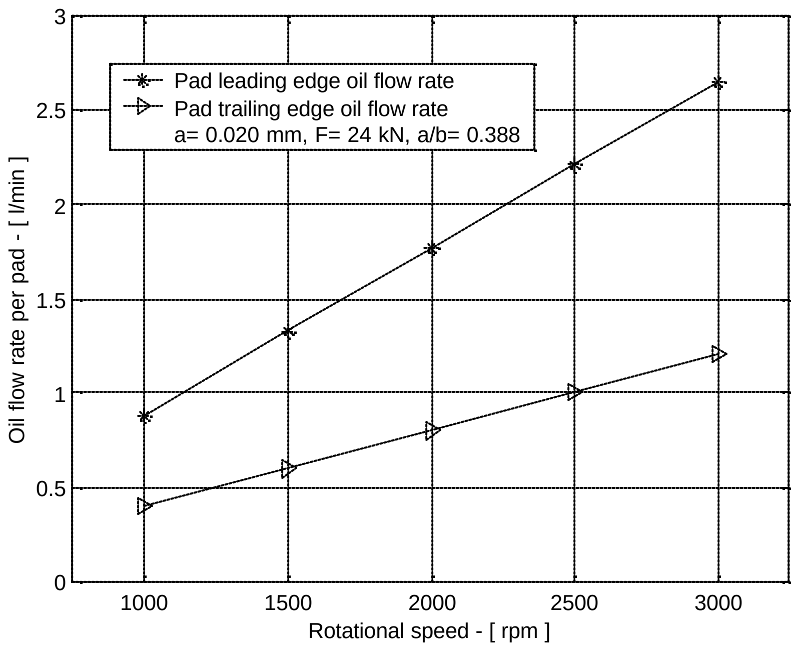

Figure 5. Computed oil flow rate at the leading and the trailing edge of a bearing pad versus the rotational speed.

4. The test module

A full description of the test rig and instrumentation is given by Schwarz et all (2002). The test module itself is shown in Fig. (6) and consists mainly by the drive spindle (19), rotating collar (16) tilting pads (14), leveling plates (13) base ring (12) and oil reservoir (15). The additional ring (12A) was installed between the base ring and the oil reservoir, in order to drive in a more effective way the supplied oil through six radial channels existing in the bottom of the base ring. In this way, the supplied oil is driven from the outer to the inner radii of the base ring and then it flows radially from the inner to the outer radii of the pads, through the six radial channels existing between them. In some tests, the ring (12B) was addapted to the base ring (12), in order to reduce oil churning around the rotating collar (16 and 17), a sufficient clearance of about *1 mm* being maintained between the rotating collar and the additional ring (12B).

Thrust load is applied through an hydraulic jack positioned just below the load cell (01), which measures the load, that is transferred to the base ring and the tilting pads through the three vertical rods (04). In this way, the load is applied upwards from the pads against the rotating collar. An ISO VG32 mineral oil with viscosities of 27.2 mPa.s at 40^0C and 4.6 mPa.s at 100^0C. Bearing friction torque was measured through an HBM T10F torquemeter, which access the total torque from both the tilting pad thrust bearing itself, and two rolling contact bearings that counteracts the applied thrust load as well as give support to the drive spindle. Temperature measurement was accomplished by using type K (chromel/alumel) theromcouples embedded at several positions within the collar and two pads. Also, the temperatures of the oil supplied to the bearing assembly at the inlet and outlet positions in the reservoir are measured through two thermocouples conveniently installed at the inlet and outlet oil lines. For most of the tests, the lubricant oil was supplied at 45^0C, although some tests were effected with inlet oil temperatures from 40^0C to 65^0C in steps of 5^0C.

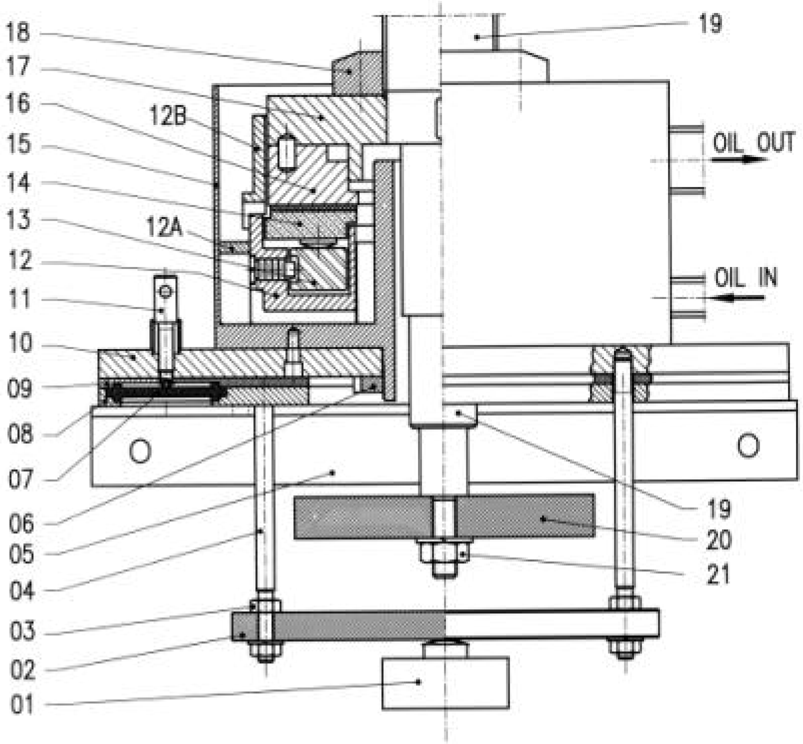

Figure 6. Details of the thrust bearing and loading system.

5. Experimental Results

The experimental results were obtained for three different tilting pad bearings consisted by six sector shaped pads with pivots positioned at 50%, 60% and 66% of the pad mean circumferencial length, respectively. Rotational speeds varied from 500 to 3500 rpm, applied load from 12 to 24 kN and supplied oil flow rate from 1.7 to 9 l/min. The presentation and discussion of the results is made on the basis of Fig. (7), which shows the thermocouple positions (dimensions in mm) whithin the collar and a pad. A photograph of a 66% pivoted pad, prepared for thermocouple insertions, is also shown in the figure. The collar positions are indicated by C1, C2, C3, C4, C5 and C6, while the pad positions are indicated by S4 to S16. Positions 1, 2, 3 and 9 are indicated without the prefix S in cross section AA, due to lack of space. Two pads were instrumented, such that thermocouples S14, S15, and Sl6 were positioned in the second pad and measure the oil temperatures at the leading edge, outer radius and the trailing edge of the pad, respectively. Two additional thermocouples in positions S5 and S13 are repeated in both pads, enabling a comparison among the corresponding temperatures.

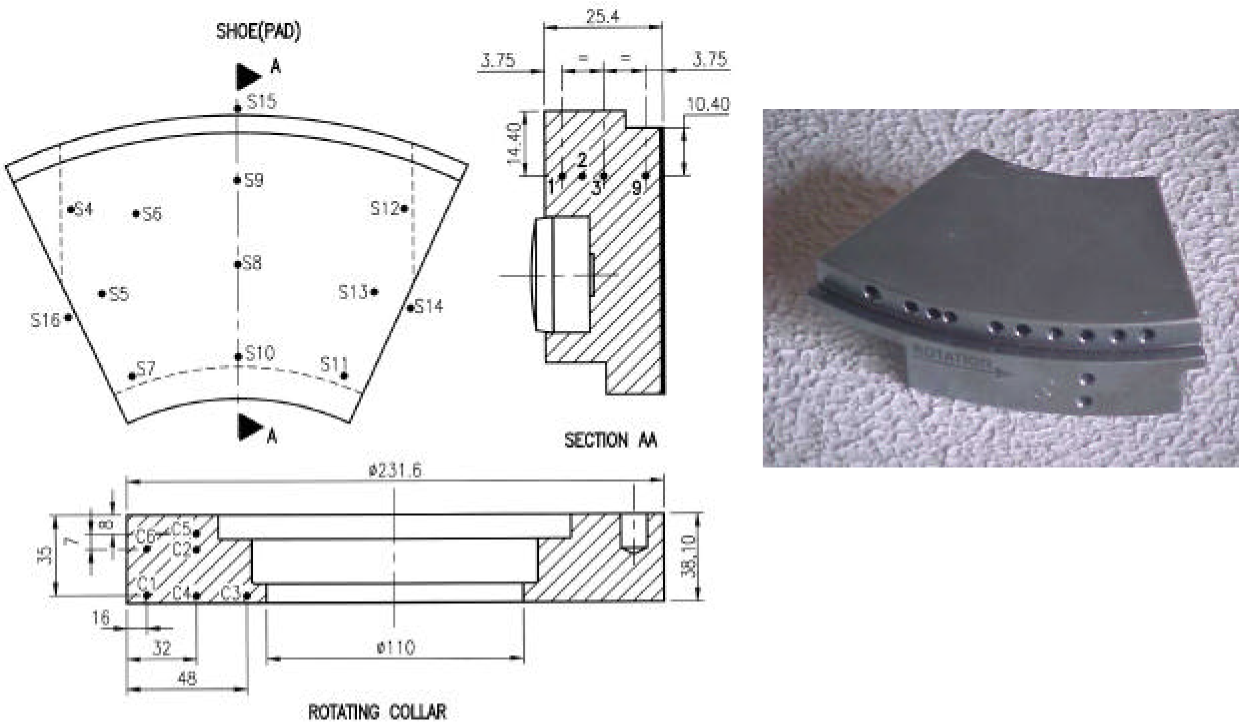

Figure 7. Thermocouple positions within the collar and a pad.

Table (2) shows the steady state temperatures for a 21 kN thrust load and at 2500 rpm, for the 6 positions within the collar and 18 positions within the two pads for the three thrust bearings, i. e., with centrally pivoted pads, pads with pivots at 60% and 66% of the circumferencial length, respectivelly. Three additional thermocouples give the ambient temperature, *Ta*, the oil supply temperature, *Ti*, and the outlet oil temperature, *To*. Note that in Tab. (2) the five themocouples positioned in the second pad are denoted by an asterisc (*). Steady state friction torques are also given in Tab. (2) for the three bearings.

Table 2. Temperature distributions within the pads and collar, for the pads with three different pivot positons.

Rotational speed: 2500 rpm Axial Load: 21 kN				Lubricating Oil ISO 32 Oil Flow rate: 1,9 (l/min.)				Pivot position: 50% 60% 66% Friction Torque: 8.47 7,68 7,53 (N.m)			
Temperatures ^{o}C											
Pos.	Pivot position			Pos.	Pivot position			Pos.	Pivot position		
	50%	60%	66%		50%	60%	66%		50%	60%	66%
S1	94.2	-	86.9	S2	95.8	-	88.5	S3	96.2	-	88.5
S4	99.9	94.5	91.6	S5	99.7	93.8	91.1	S7	94.6	90.6	88.7
S8	100.7	92.5	88.5	S9	100.2	92.6	88.3	S10	96.5	89.9	86.7
S11	91.5	85.6	83.0	S12	93.0	84.0	81.7	S13	-	85.8	82.9
S14*	86.3	79.9	79.5	S15*	86.9	81.4	80.2	S16*	86.8	81-86	88.5
C2	103.2	94.4	95.0	C4	106.3	98.3	97.2	C5	101.2	93.2	92.7
C1	102.6	93.8	94.5	C3	103.5	95.7	94.8	C6	97.8	90.4	88.9
Ta	22.0	24.3	26.6	Ti	45.0	45.0	45.2	To	79.0	78.0	76.6
S6	100.8	94.4	91.4	S5*	97.5	91.1	90.5	S13*	91.3	84.0	81.5

* thermocouples embedded in a second pad

Ta = ambient air temperature; Ti = inlet oil temperature; To = outlet oil temperature.

It can be concluded from Tab. (2) that the steady state temperatures and friction torques were about 8% and 11% lower for the 60% and the 66% pivoted pads, respectively, as compared to the bearing with centrally pivoted pads.

It may also be seen from Tab. (2) that the temperatures corresponding to positions S6 or S4 and S12 were, respectively, the maximum and minimum pad temperatures. Further, it can be noted that the temperatures corresponding to positions S4, S5 and S6 are essentially the same, for the three bearings.

Another evidence from Tab. (2) is that, for the two offset pivoted pads, the temperatures S4 were slightly higher than the temperatures S6. However, for the bearing consisted by six centrally pivoted pads, the maximum temperature occurs in position S6, i.e., at 75% of the pad radial length and at 75% of the pad arc length, in the direction of rotation, as had also been obtained by Gregory (1974), from a horizontal shaft thrust bearing.

Also, from the collar and pads temperatures near the "contact" surface, it is observed that the collar temperature is about 5% to 6% higher than the pad surface temperature.

From the collar and pad axial temperature gradients given in Tab. (2) and by applying the basic conduction heat transfer equations, it may be concluded that about 40% of the bearing friction power loss are transferred to the collar and to the pads, in general agreement with the distribution proposed by El-Saie & Fenner (1988).

Figure (8) shows, for the 66% offset pivoted pads, the variation of temperatures S4 and S12 and the friction torque with the oil flow rate supplied to the bearing. As expected, friction torque increases significantly with oil flow rate, while the temperatures decrease. It can be observed that the difference between the temperatures S4 and S12 remains almost constant as the oil flow rate is increased. Also, the operating steady state temperatures remain almost constant for oil flow rates above 7.0 l/min, but the bearing friction torque continues to increase, however less significantly. Therefore, for the operating conditions indicated in Fig. (8), the supplied oil flow rate of about 7.0 to 8.0 l/min may be considered as the ideal value from the standpoint of minimal operating temperature condition. Increasing the oil flow rate to values above 8.0 l/min will only produce higher power losses in the bearing, without lowering the operating temperatures. As was to be expected, for slower rotational speeds, such an ideal oil flow rate is lower, e.g., about 5.0 to 6.0 l/min for 1500 rpm.

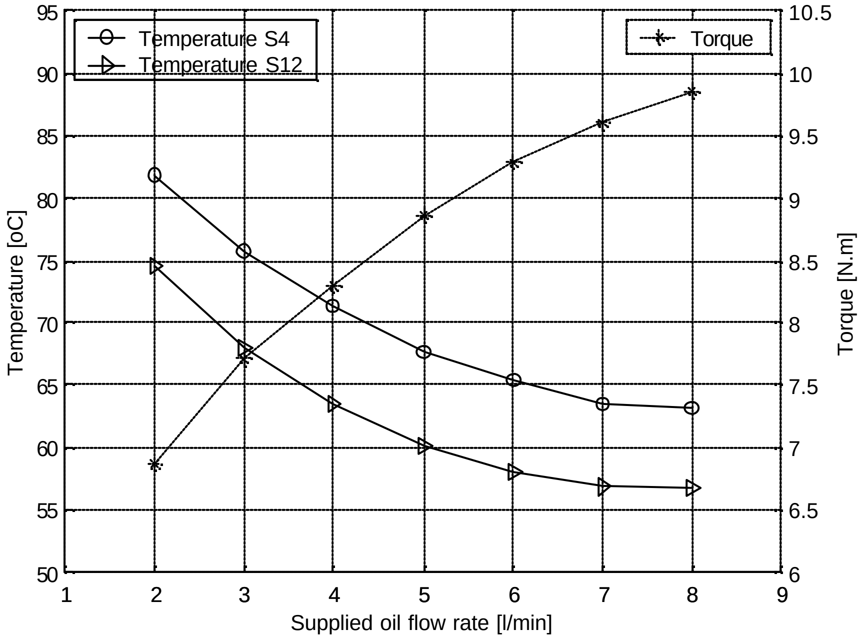

Figure 8. Variation of temperatures and torque with supplied oil flow rate, for 2000 rpm and 18 kN thrust load.

The test-rig has not yet been instrumented for measurement of the oil film thickness between each pad and the rotating collar. This is one of the next steps in the present research program. However, a rough estimative of the minimum oil film thickness may be obtained from a comparative analysis between the experimentally obtained friction torque given in Fig. (8), for the 66% pivoted pad, and the theoretical value from Fig. (2), for a taper ratio a/b = 0.4, for a 18 kN thrust load and 2000 rpm, as follows. For example, considering the "ideal" 7.0 l/min oil flow rate supplied to the bearing, the experimental friction torque from Fig. (8) is about 9.6 N.m and, for this value, the corresponding minimum oil film thickness is about 36 μm, as may be obtained from Fig. (2).

Figure (9) shows how significantly the oil supply temperature affects the operating torque and pad temperatures, for the pads pivoted at 66% of the sector angle, 18 kN thrust load, 2500 rpm, 5.0 l/min oil flow rate and for a 25^0C ambient temperature. It can be seen that a 5^0C increase in the temperature of the oil supplied to the bearing, causes a bearing temperature rise of about 5% and a friction torque decrease of about 5%.

6. Conclusions

From the theoretically simulated results it was concluded that the sector pads pivoted at about 66% of the sector angle leads to minimum power loss in the bearing. This was experimentally confirmed from the data in Tab. (2), which shows that the steady state temperatures and friction torques were about 8% and 11% lower for the 60% and the 66% pivoted pads, respectively, as compared to the bearing with centrally pivoted pads.

The temperature of the collar at the mean diameter is about 3% above the temperatures at the 22% and 72% of the radial width. Therefore, the collar surface temperature distribution may no longer be assumed as uniform over the whole "contact" surface.

For a given condition of speed and thrust load, there is an ideal oil flow rate to be supplied to the bearing, in order to obtain minimum working temperatures, without unnecessary increase in power losses.

The temperature of the oil supplied to the bearing has a significant effect on its behavior. The higher the supply temperature, the lower the friction torque and the higher the bearing operating temperatures.

Friction torque is significantly affected by oil flow rate, oil supply temperature and particular details of the whole bearing assembly. For example, some test runs were performed with the ring 12B, Fig. (6) adapted to the base ring 12, aiming to reduce oil churning. A friction torque increase of about 10% was observed, corresponding very closely to the well known Petroff´s torque from the shearing of the oil film between two concentric cylinders.

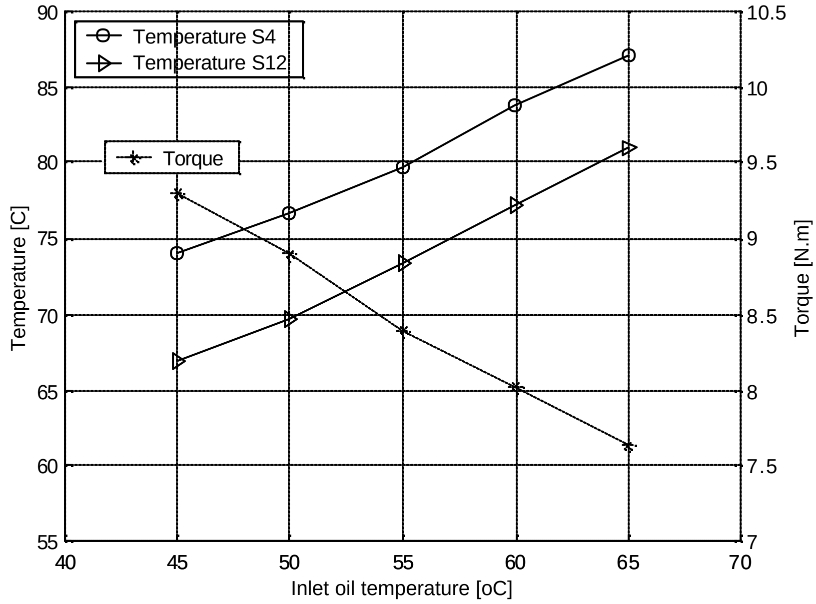

Figure 9. Operating temperatures and friction torque versus the temperature of the oil supplied to the bearing.

4. Acknowledgement

The authors gratefully acknowledge the financial support from FAPEMIG – Fundação de Amparo à Pesquisa do Estado de Minas Gerais, Proc. TEC 855/97 and technical and financial support from Kingsbury Inc.

5. References

Ali El-Saie, Y.M.H. and Fenner, R.T., 1988, “Three-Dimensional Thermo- Elastohydrodynamic Analysis of Pivoted Pad Thrust Bearings. Part 1: Treatment of Bearing Deflections and Fluid Film Flow and Heat Transfer”, Proc. Inst. Mech. Eng., Vol.202, pp.39-50.

Ali El-Saie, Y.M.H. and Fenner, R.T., 1988, “Three-Dimensional Thermo- Elastohydrodynamic Analysis of Pivoted Pad Thrust Bearings. Part 2: Application of Theory, Comparaison with Experiments”, Proc. Inst. Mech. Eng., Vol.202, pp.51-62.

Almqvist, T., Glavatskikh, S.B. and Larsson, R., 2000, “THD Analysis of Tilting Pad Thrust Bearings-Comparison Between Theory and Experiments”, ASME Trans., Journal of Tribology, Vol. 122, pp. 412-417.

Dadouche, A. Fillon, M. and Bligoud, J.C., 2000, “Experiments on Thermal Effects in a Hydrodynamic Thrust Bearing”, Tribology International,Vol. 33, pp. 167-174.

Glavatskikh, S.B., 2001, “Steady State Performance Characteristics of a Tilting Pad Thrust Bearing”, Trans. ASME, Journal of Tribology, Vol. 123, pp. 608-615.

Gregory, R.S., 1974, “Performance of Thrust Bearings at High Operating Speeds”, J. Lubr. Technol., Vol. 96, No. 1, pp. 7-14.

Mikula. A.M., 1987, “The Effect of Lubricant Supply Temperature ou the Thrust Bearing Performance”, ASLE Trans., 30, No. 2, pp. 220-224.

Salles, W. J., Mouallem, G. E., Schwarz, V.A. and Manzanares, N., 2001, “Solución Numerica De La Ecuación de Reynolds para Cojinetes Axiales de Patines Sectoriales”, Información Tecnologica, Vol. 12, No. 2, La Serena, Chile, pp. 127-134.

Schwarz, V.A., Silva, P.F., Dias, J.C., Salles, W.J. and Wilkes, J.,2002, “Experimental Analysis of Thermal Effects on Tilting Pads Hydrodynamic Thrust Bearings – On the Search for Minimum Power Loss Conditions”, 9th Brazilian Congress of Thermal Engineering and Sciences, Caxambu – MG, pp. 1-11.